Polymer Chemistry

Accepted Manuscript

ROYAL SOCIETY OF CHEMISTRY

www.rsc.org/polymers

Poly(methacrylic acid)-based AB and ABC Block Copolymer Nano-Objects prepared via RAFT Alcoholic Dispersion Polymerization

M. Semsarilar, V. Ladmiral, A. Blanazs and S. P. Armes*

Department of Chemistry, The University of Sheffield, Brook Hill, Sheffield, S3 7HF, UK

* Corresponding author. Email: s.p.armes@sheffield.ac.uk; Tel: +44 (0)1142 229342; Fax: +44 (0)1142 229346

Abstract. A series of well-defined amphiphilic poly(methacrylic acid)-poly(benzyl methacrylate) (PMAA-PBzMA) diblock copolymers are synthesized via polymerization-induced self-assembly using an alcoholic dispersion polymerization formulation. Chain growth is mediated via reversible addition-fragmentation chain transfer polymerization (RAFT) chemistry using a trithiocarbonate-based chain transfer agent (CTA) at 70°C. The poly(methacrylic acid) block is soluble in ethanol and acts as a steric stabilizer for the growing insoluble PBzMA chains, resulting in the *in situ* generation of diblock copolymer nano-objects in the form of spheres, worms or vesicles, depending on the precise reaction conditions. Copolymer morphologies can be covalently stabilized via cross-linking to prevent their dissociation when transferred into aqueous solution, which leads to the formation of highly anionic nano-objects due to ionization of the PMAA stabilizer chains. ABC triblock copolymer nanoparticles can also be prepared using this approach, where the third block is based on the semi-fluorinated monomer, 2,2,2-trifluoroethyl methacrylate (TFEMA). GPC studies confirm that chain extension is efficient and high TFEMA conversions can be achieved. Internal phase separation between the mutually incompatible PBzMA and semi-fluorinated PTFEMA core-forming blocks occurs, producing a range of remarkably complex semi-fluorinated triblock copolymer morphologies.

---

* Author to whom correspondence should be addressed (s.p.armes@shef.ac.uk)

Introduction

The development of living radical polymerization techniques over the last two decades has revolutionized synthetic polymer chemistry.[1-14] A wide range of functional monomers can now be polymerized with good control and many different copolymer architectures can be accessed, including well-defined macromonomers, star copolymers, branched copolymers and block copolymers.[15-18] In the latter case, AB diblock copolymers are usually synthesized in a good solvent for both blocks, with the final desired copolymer morphology being achieved via post-polymerization processing in either solution or the solid state.[19-23] However, recent research suggests that polymerization-induced self-assembly (PISA) offers an efficient and highly attractive route for the *direct* synthesis of a range of diblock copolymer nano-objects.[24-50] Such formulations are typically based on reversible addition-fragmentation chain transfer (RAFT) polymerization,[1-4] which is conducted under either aqueous emulsion [24-33] or dispersion [34-50] polymerization conditions. In the latter case, the continuous phase may be water, [35-40, 43, 45, 46] alcohol [34, 41, 42, 44, 47-50] or *n*-alkanes,[51,52] which underlines the versatility of this PISA approach.

Several groups have reported alcoholic dispersion polymerization formulations based on RAFT chemistry. For example, Pan et al. has polymerized styrene using various macromolecular chain transfer agents (macro-CTAs) using RAFT chemistry.[47-50] However, styrene conversions are typically substantially incomplete, even after conducting the polymerization for several days at 80°C. In contrast, very high conversions can be achieved for the core-forming block if styrene is replaced with benzyl methacrylate (BzMA), as described by Charleux et al.[32,34] and our own group.[41,42,44] Moreover, depending on the precise reaction conditions, pure phases of well-defined spheres, worms or vesicles can be obtained.[24,25,41,42,44] However, reproducible syntheses generally require construction of a detailed phase diagram for a given mean degree of polymerization for the macro-CTA, which acts as a stabilizer block.[41,42,44] The two key variables for such phase diagrams are the mean degree of polymerization for the insoluble block and the total solids concentration at which the PISA synthesis is conducted.

The macro-CTA can be prepared using non-ionic, cationic, anionic or zwitterionic monomers.[41,42] Transfer of the nano-objects from alcohol to water can lead to either colloidally stable or flocculated dispersions, depending on the precise nature of the stabilizer block.[41,42,44] In the case of macro-CTAs based on weak polyelectrolytes such as poly(methacrylic acid)

(PMAA), RAFT alcoholic dispersion polymerization offers a potentially decisive advantage over the analogous aqueous dispersion polymerization formulation, since self-assembly can be impeded in the latter case by lateral electrostatic repulsion between highly charged stabilizer chains located in the coronal layer.[38,43] In contrast, the PMAA macro-CTA remains in its neutral form when dissolved in alcohol, which facilitates the PISA synthesis. On transferring the resulting PMAA-stabilized diblock copolymer nano-objects into water, they become highly anionic at or above neutral pH due to extensive ionization of the PMAA chains.[41]

Herein we expand on our recent communication describing the synthesis of PMAA-PBzMA diblock copolymer nano-objects in ethanol via RAFT-mediated PISA at 70°C.[41] Moreover, we explore the feasibility of preparing well-defined ABC triblock copolymers from these diblock precursors via chain extension using 2,2,2-trifluoroethyl methacrylate (TFEMA), a well-known semi-fluorinated monomer (Scheme 1). [53-57]

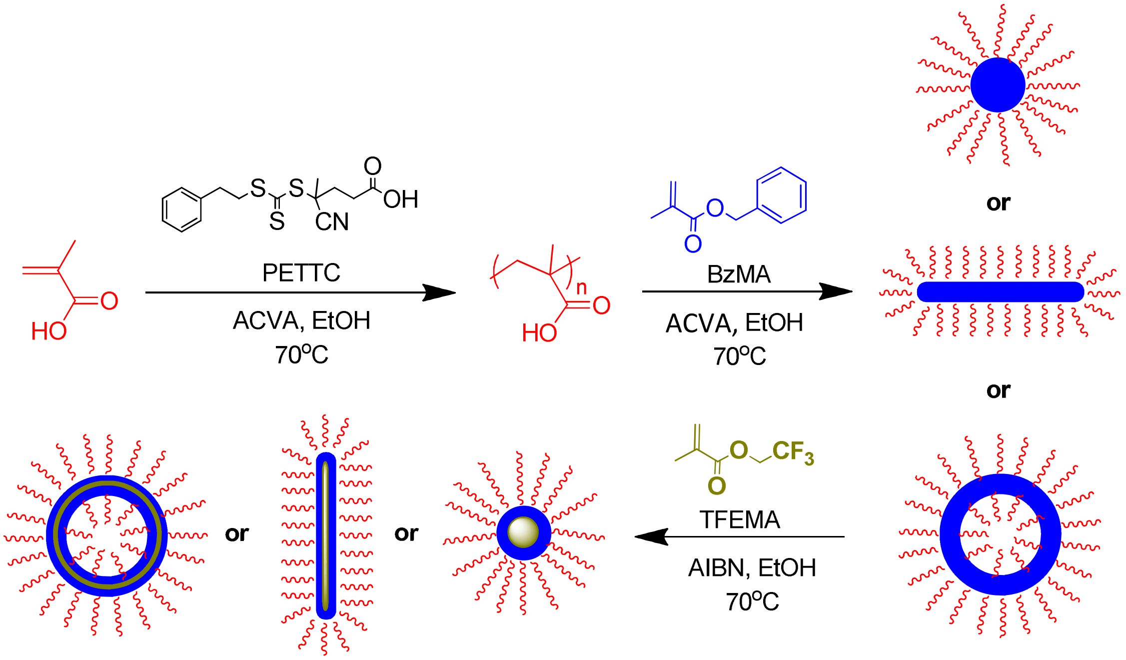

Scheme 1. RAFT synthesis of poly (methacrylic acid)-based diblock and triblock copolymer nano-objects prepared by alcoholic dispersion polymerization of first BzMA and then TFEMA monomer at 70 °C.

Experimental

Materials. All reagents were purchased from Sigma-Aldrich and were used as received unless otherwise noted. 4,4'–Azobis-4-cyanopentanoic acid (ACVA) was used as initiator. Benzyl methacrylate (BzMA, 96%) was passed through a column of inhibitor remover prior to use.

Copolymer characterization. Copolymer molecular weight distributions were assessed using size exclusion chromatography (SEC). The experimental set-up comprised two 5 µm (30 cm) Mixed C columns; a WellChrom K-2301 refractive index detector operating at 950 ± 30 nm, THF eluent containing 2.0 % v/v triethylamine and 0.05 % w/v butylhydroxytoluene (BHT) at a flow rate of 1.0 mL min^{-1}; A series of ten near-monodisperse poly(methyl methacrylates) (M_p ranging from 1,280 to 330,000 g mol^{-1}) were purchased from Polymer Labs (UK) and employed as linear calibration standards with the above refractive index detector.

Proton NMR spectra were acquired with a Bruker 250 MHz or 400 MHz spectrometer using either $CDCl_3$ or CD_2Cl_2 as the deuterated solvent. All chemical shifts are reported in ppm (δ). TEM studies were conducted using a Philips CM 100 instrument operating at 100 kV. To prepare TEM samples, 5 µL of a dilute aqueous copolymer solution was placed onto a carbon-coated copper grid, stained with uranyl formate and dried under ambient conditions. DLS studies were conducted using a Malvern Instruments Zetasizer Nano series instrument equipped with a 4 mW He-Ne laser operating at 633 nm, an avalanche photodiode detector with high quantum efficiency, and an ALV/LSE-5003 multiple tau digital correlator electronics system. Aqueous electrophoresis measurements were performed on 0.01 % w/v aqueous copolymer solutions using the same Zetasizer Nano series instrument. The solution pH was adjusted by the addition of 0.01 M HCl or 0.01 M KOH using an autotitrator.

Synthesis of 4-cyano-4-(2-phenylethanesulfanylthiocarbonyl) sulfanylpentanoic acid (PETTC)

2-Phenylethanethiol (10.5 g, 76.0 mmol) was added over 10 min to a stirred suspension of sodium hydride (60% in oil) (3.15 g, 79.0 mmol) in diethyl ether (150 mL) at 5-10 ˚C. A vigorous evolution of hydrogen was observed and the grayish suspension turned into a thick white slurry of sodium phenylethanethiolate over 30 minutes. The reaction mixture was cooled to 0 ˚C and carbon disulfide (6.00 g, 79.0 mmol) was gradually added to produce a thick yellow precipitate of sodium 2-phenylethanetrithiocarbonate, which was collected by filtration after 30 minutes and used in the next step without purification.

Solid iodine (6.30 g, 25.0 mmol) was gradually added to a suspension of sodium 2-phenylethanetrithiocarbonate (11.6 g, 4.09 mmol) in diethyl ether (100 mL). The reaction mixture was then stirred at room temperature for 1 h and the white sodium iodide was removed by filtration. The yellow–brown filtrate was washed with an aqueous solution of sodium thiosulfate to remove excess iodine, dried over sodium sulfate and then evaporated to leave a solid residue of bis-(2-phenylethanesulfanylthiocarbonyl) disulfide (~100% yield). A solution of 4,4'-azobis(4-cyanopentanoic acid) (ACVA; 2.10 g, 75.0 mmol) and bis-(2-phenylethane sulfanylthiocarbonyl) disulfide (2.13 g, 5.0 mmol) in ethyl acetate (50 mL) was degassed via nitrogen bubbling and then heated at reflux under N_2 atmosphere for 18 h. After removal of the volatiles under vacuum, the crude product was washed with water (5 x 100 mL). The organic phase was concentrated and purified by silica column (initially 7:3 petroleum ether: ethyl acetate, gradually increasing to 4:6) to afford 4-cyano-4-(2-phenylethane sulfanylthiocarbonyl) sulfanylpentanoic acid as a yellow oil (78% yield).

^{1}H NMR (400.13 MHz, CD_2Cl_2, 298 K) δ (ppm) = 1.89 (3H, $-CH_3$), 2.34-2.62 (m, 2H, $-CH_2$), 2.7 (t, 2H, $-CH_2$), 3.0 (t, 2H, $-CH_2$), 3.6 (t, 2H, $-CH_2$), 7.2-7.4 (m, 5H, aromatic).

^{13}C NMR (400.13 MHz, CD_2Cl_2, 298 K) δ (ppm) = 24.2 (CH_3), 29.6 ($CH_2\mathit{CH_2}COOH$), 30.1($\mathit{CH_2}Ph$), 33.1 ($\mathit{CH_2}$ CH_2COOH), 39.9 ($S\mathit{CH_2}CH_2Ph$), 45.7 ($S\mathit{C}CH_2$), 118.6 (CN), 127.4, 128.8, 129.2, 144.3 (Ph), 177.4 (C=O), 222.2 (C=S).

Synthesis of poly(methacrylic acid) (PMAA) macro-CTA agent

In a typical synthesis, a round-bottomed flask was charged with MAA (5.00 g; 58.0 mmol), PETTC (300 mg; 0.890 mmol), ACVA (50.0 mg, 0.179 mmol; CTA/initiator molar ratio = 4.97) and ethanol (5.00 g). The sealed reaction vessel was purged with nitrogen and placed in a pre-heated oil bath at 70˚C for 3 h. The resulting PMAA macro-CTA (MAA conversion = 100 %; after methylation, M_n = 9,000 g mol^{-1}, M_w = 11,000 g mol^{-1}, M_w/M_n = 1.19) was purified using dialysis, first against a 1:1 water: methanol mixture and then against pure deionized water. The polymer was isolated by lyophilization. A mean DP of 70 was calculated for this macro-CTA using ^{1}H NMR by comparing the integrated signal intensity due to the aromatic protons at 7.2-7.4 ppm with that due to the methacrylic polymer backbone at 0.4-2.5 ppm.

Synthesis of linear poly (methacrylic acid)-poly (benzyl methacrylate) (PMAA-PBzMA) diblock copolymer nanoparticles via dispersion polymerization in ethanol

The following alcoholic dispersion polymerization protocol conducted at 20 % w/w solids and targeting $PMAA_{70}$-$PBzMA_{100}$ is typical. BzMA (1.00 g; 5.70 mmol), ACVA (1.59 mg; 0.006 mmol; CTA/initiator molar ratio = 4.67) and $PMAA_{70}$ macro-CTA (0.170 g; 0.028 mmol) were dissolved in ethanol (4.70 g). The reaction mixture was sealed in a round-bottomed flask, purged with nitrogen for 15 min. and then placed in a pre-heated oil bath at 70˚C for 24 h.

Synthesis of cross-linked poly (methacrylic acid)-poly (benzyl methacrylate)-poly (ethylene glycol dimethacrylate) (PMAA-PBzMA-PEGDMA) triblock copolymer nanoparticles

The following alcoholic dispersion polymerization protocol conducted at 20 % w/w solids and targeting $PMAA_{70}$-$PBzMA_{100}$–$PEGMA_{10}$ is typical. BzMA (0.60 g; 3.40 mmol), ACVA (1.00 mg; 0.003 mmol; CTA/initiator molar ratio 5.67) and $PMAA_{70}$ macro-CTA (98.0 mg; 0.017 mmol) were dissolved in ethanol (3.10 g). The reaction mixture was sealed in a round-bottomed flask, purged with nitrogen for 15 min. and then placed in a pre-heated oil bath at 70˚C for 14 h (97 % conversion). In a separate vial, EGDMA (65.0 µL, 0.340 mmol) was degassed alongside ACVA (0.300 mg, 0.110 mmol) and this mixture was transferred under nitrogen to the reaction vessel. The reaction solution was stirred for a further 17 h at 70˚C (100 % conversion, as judged by ^{1}H NMR).

Synthesis of poly (methacrylic acid)-poly (benzyl methacrylate)-poly (ethylene glycol dimethacrylate) (PMAA-P(BzMA-stat-EGDMA)) diblock copolymer particles

The following alcoholic dispersion polymerization protocol conducted at 20 % w/w solids and targeting $PMAA_{70}$-P($BzMA_{100}$-stat-$PEGMA_{10}$) is typical. BzMA (0.60 g; 3.40 mmol), EGDMA (65.0 µL, 0.340 mmol), $PMAA_{70}$ macro-CTA (98.0 mg; 0.017 mmol) and ACVA (1.00 mg; 0.003 mmol; CTA/initiator molar ratio 5.67) were dissolved in ethanol (3.10 g). This reaction mixture was sealed in a round-bottomed flask, purged with nitrogen for 15 minutes and then placed in a pre-heated oil bath at 70˚C for 24 h.

Synthesis of poly (methacrylic acid)-poly (benzyl methacrylate)-poly (2,2,2-trifluoroethyl) methacrylate) (PMAA-PBzMA-PTFEMA) triblock copolymer particles

The following alcoholic dispersion polymerization protocol conducted at 20 % w/w solids and targeting $PMAA_{70}$-$PBzMA_{100}$ is typical. BzMA (0.60 g; 3.40 mmol), $PMAA_{70}$ macro-CTA (0.21 g; 0.034 mmol) and ACVA (2.00 mg; 0.006 mmol; CTA/initiator molar ratio 5.67) were dissolved in ethanol (3.20 g). This reaction mixture was sealed in a round-bottomed flask, purged with nitrogen for 15 min. and then placed in a pre-heated oil bath at 70˚C for 14 h (~ 100 % conversion, as judged by ^1H NMR). In a separate vial, TFEMA (1.72 g, 10.22 mmol) and AIBN (2.24 mg, 0.014 mmol) were degassed in ethanol (6.90 g). This monomer/initiator mixture was transferred under nitrogen to the reaction vessel. The polymerizing mixture was stirred at 70˚C for a further 24 h (~ 100 % conversion, as judged by ^1H NMR).

Chemical Derivatization of Copolymers for SEC Analysis

For size exclusion chromatography, the polymers were modified by methylation of the carboxylic acid groups on the PMAA block using excess trimethylsilyldiazomethane, as reported by Couvreur *et al*.[58] Briefly, 50 mg of each copolymer was dissolved in THF and a yellow solution of trimethylsilyldiazomethane was added dropwise at 20^{o}C. Upon addition, effervescence was observed and the solution immediately became colorless. Addition of trimethylsilyldiazomethane was continued until the solution became yellow and effervescence ceased. Then, a small excess of trimethylsilyldiazomethane was added and the solution was stirred for a further 6 h at 20^{o}C. Full methylation of the methacrylic acid residues was confirmed by ^1H NMR spectroscopy

Results and Discussion

We have previously reported that the synthesis of poly(methacrylic acid)-poly(benzyl methacrylate) diblock copolymer nano-objects using a PMAA macro-CTA for the RAFT alcoholic dispersion polymerization of benzyl methacrylate can produce various copolymer morphologies, depending primarily on the mean degree of polymerization of the core-forming PBzMA block.[41]

First, a series of *spherical* $PMAA_{70}$-$PBzMA_x$ particles were prepared at various copolymer concentrations. As reported previously by both Li et al.[35] and Jones et al.,[42] the hydrodynamic diameter of such diblock copolymer nanoparticles can be readily tuned by varying the DP of the core-forming block. At 5 % w/w solids, the mean particle diameter can be systematically increased from 52 nm to 133 nm by varying the target DP of the PBzMA from 29 to 194. In each case the particle size distribution remains relatively narrow, as judged by DLS. A similar monotonic increase in particle diameter is observed for diblock copolymer syntheses conducted at 10, 15 or 20 % solids up to the point where a mixed phase of spheres and worms is produced. These results are summarized in Table 1 and Figure 1.

Table 1. Summary of DLS hydrodynamic diameters for $PMAA_{70}$-$PBzMA_x$ spherical nanoparticles

Solids Content [a]	**Targeted DP_{PBzMA}**	**Conv.%**	**Actual DP of PBzMA** [b]	**d (nm)** [c]	**PDI**
5	30	98	29	52	0.09
5	50	100	50	61	0.03
5	70	96	67	74	0.03
5	90	93	84	84	0.06
5	100	98	98	90	0.05
5	150	100	150	110	0.03
5	200	97	194	133	0.02
10	50	85	43	51	0.04
10	70	94	66	60	0.02
10	90	99	89	72	0.01
15	50	90	45	55	0.03
15	70	85	60	63	0.05
15	90	95	86	73	0.03
20	50	95	48	57	0.02
20	70	94	66	67	0.02
20	90	94	85	76	0.07

[a] % w/w.
[b] Determined by ^1H NMR spectroscopy.
[c] Intensity-average hydrodynamic diameter reported by dynamic light scattering (DLS).

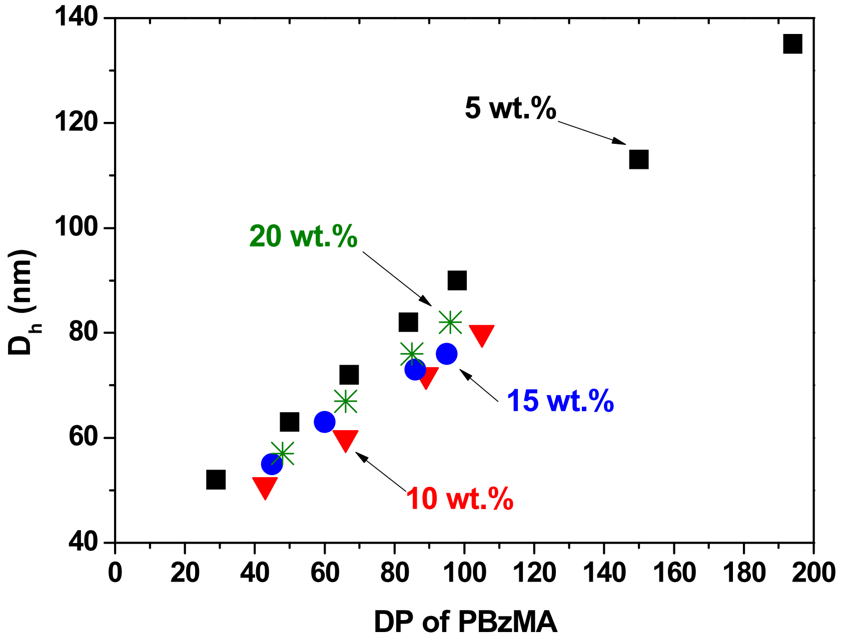

Figure 1. Relationship between the DLS hydrodynamic diameter and DP of the core-forming PBzMA block for $PMAA_{70}$-$PBzMA_x$ spherical diblock copolymer nanoparticles prepared via RAFT alcoholic dispersion polymerization at 5 (black squares), 10 (red triangles), 15 (blue circles) and 20 (green stars) % w/w solids.

These $PMAA_{70}$-$PBzMA_x$ spherical nanoparticles can be readily transferred from ethanol into aqueous media via dialysis without any loss of colloidal stability. After dialysis, the pH of the aqueous dispersion was lowered to pH 1 by addition of dilute HCl. The first equivalence point shown in Figure 2 simply corresponds to the titration of the HCl in solution. On addition of further NaOH, the PMAA stabilizer chains become ionized to produce highly anionic particles. Acid titration studies of the $PMAA_{70}$ macro-CTA (the second equivalence point) suggest a pK_a value of approximately 6.0, which is close to the pK_a values of approximately 6.2 estimated for the PMAA stabilizer chains of the diblock copolymer nano-objects (see Figure 2).

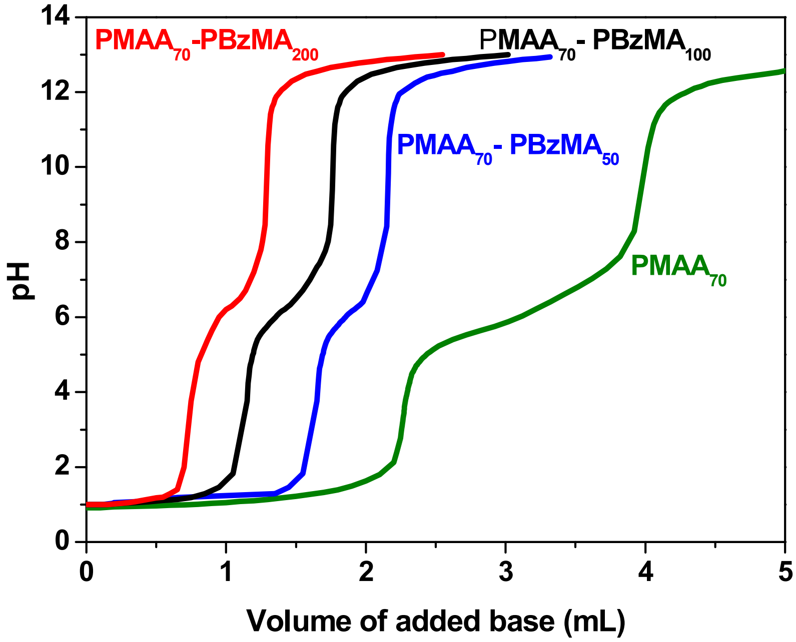

Figure 2. Acid titration curves obtained for PMAA$_{70}$-PBzMA$_x$ diblock copolymer nanoparticles in water and the corresponding PMAA$_{70}$ macro-CTA: (🟩) PMAA$_{70}$ macro-CTA; (🟦) PMAA$_{70}$-PBzMA$_{50}$ spheres; (⬛) PMAA$_{70}$-PBzMA$_{150}$ worms; (🟥) PMAA$_{70}$-PBzMA$_{200}$ vesicles.

The particle surface charge for each type of copolymer morphology was evaluated by aqueous electrophoresis, see Figure 3. All three types of particles were electrically neutral at around pH 2.5 to 3.0, since the PMAA chains have essentially non-ionic character under these conditions. As the solution pH is gradually raised the PMAA chains begin to acquire anionic character, which results in negative zeta potentials. Ionization of the stabilizer chains is complete at around pH 4 and the negative zeta potential then remains essentially constant up to pH 11.5. This generic behavior is observed for spherical, worm-like and vesicular particles. However, the limiting zeta potentials are around -35 mV, -42 mV and -48 mV for spheres, worms and vesicles respectively. The reason(s) for these subtle differences in electrophoretic behavior are not well understood. However, it seems likely that the progressive reduction in the molecular curvature from spheres to vesicles may be important, because this should lead to a somewhat thicker anionic stabilizer layer for the latter morphology.

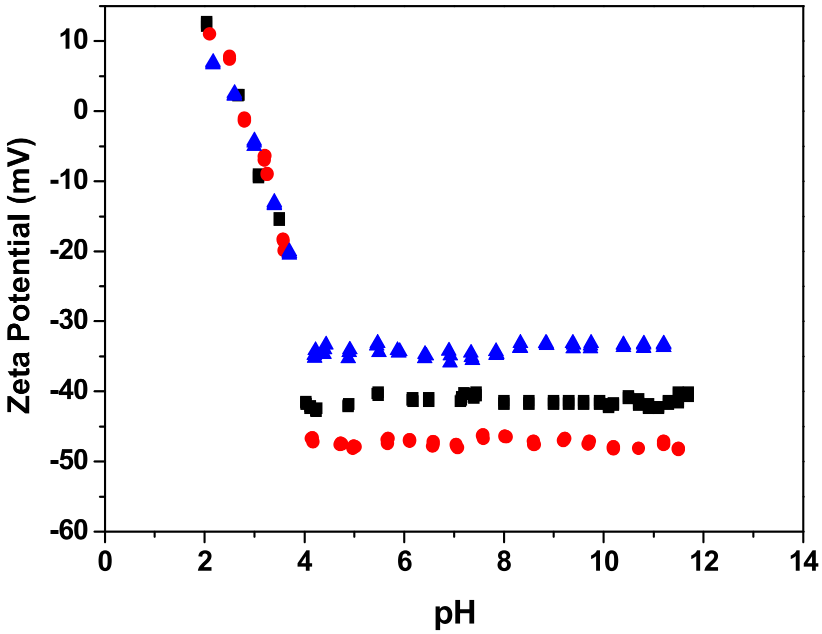

Figure 3. Zeta potential vs. pH curves obtained for three diblock copolymer morphologies: (▲) PMAA$_{70}$-PBzMA$_{50}$ spheres; (■) PMAA$_{70}$-PBzMA$_{150}$ worms; (●) PMAA$_{70}$-PBzMA$_{200}$ vesicles.

TEM studies were conducted to examine whether the copolymer morphology remained unchanged after transfer of these diblock copolymer nano-objects from ethanol into water. Copolymer dispersions that originally possessed spherical, worm-like and vesicular morphologies were diluted in water at pH 5 or pH 9 and allowed to stand at 20 ^{o}C for 4 h prior to TEM sample preparation. As shown in Figures 4d and 4g, the spherical particles remain unchanged at each pH. In the case of the worms, transfer from ethanol to an aqueous solution at pH 5 appears to cause a reduction in the mean worm length (compare Figures 4b and 4e), with shorter worms being observed at pH 9 (see Figure 4h). In the case of the vesicles (Figure 4c), transfer into water led to the appearance of a minor worm phase at pH 5, which becomes more noticeable at pH 9 (compare Figures 4f and 4i). Presumably, the greater hydrophilic character of the anionic PMAA chains causes an increase in the copolymer curvature, which leads to a change in copolymer morphology via a (partial) vesicle-to-worm transition.[59]

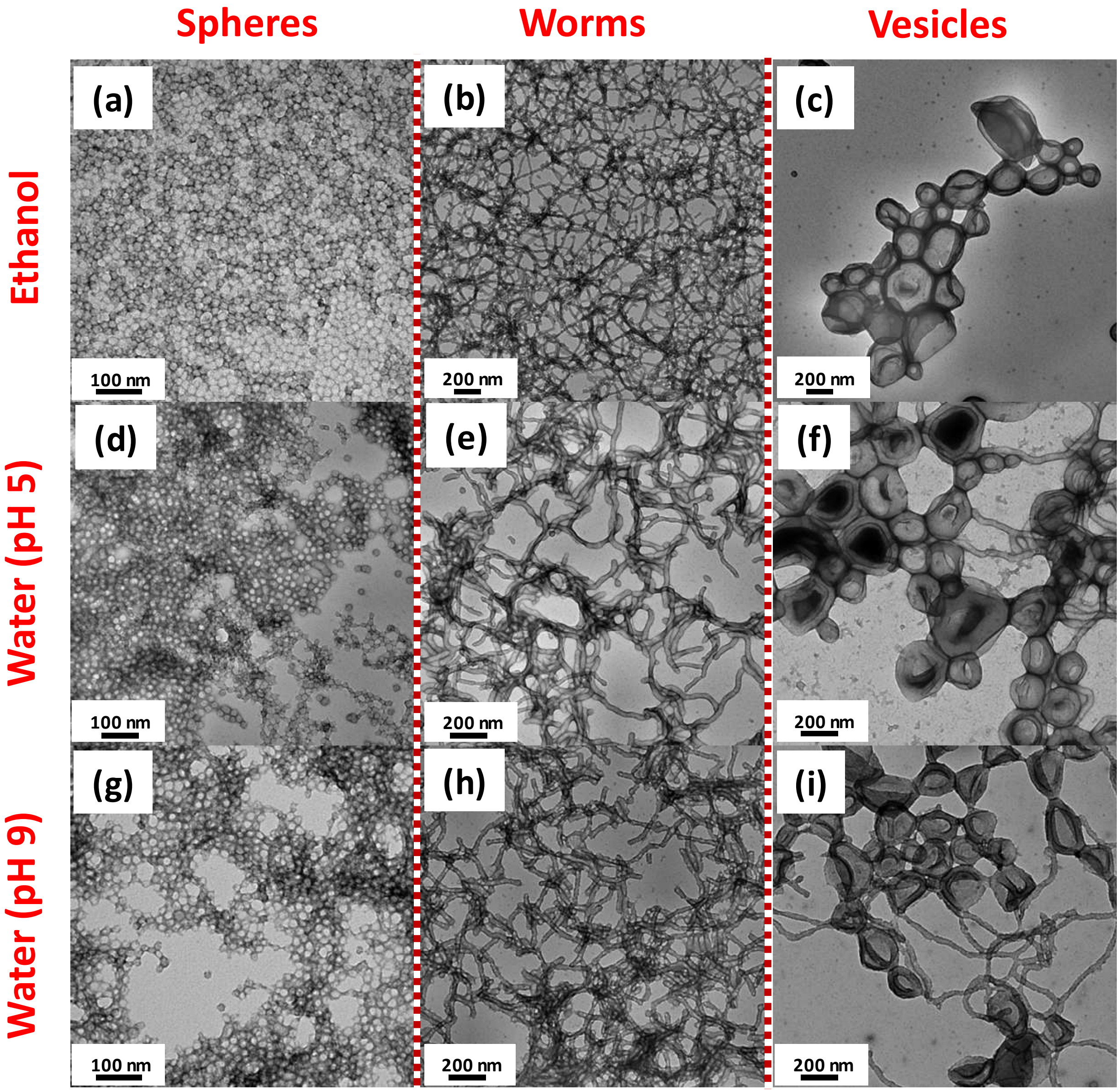

Figure 4. (a) $PMAA_{70}$-$PBzMA_{50}$ spheres in ethanol; (b) $PMAA_{70}$-$PBzMA_{150}$ worms in ethanol; (c) $PMAA_{70}$-$PBzMA_{200}$ vesicles in ethanol; (d) $PMAA_{70}$-$PBzMA_{50}$ spheres at pH 5; (e) $PMAA_{70}$-$PBzMA_{150}$ worms at pH 5; (f) $PMAA_{70}$-$PBzMA_{200}$ vesicles at pH 5; (g) $PMAA_{70}$-$PBzMA_{50}$ spheres at pH 9; (h) $PMAA_{70}$-$PBzMA_{150}$ worms at pH 9; (i) $PMAA_{70}$-$PBzMA_{200}$ vesicles at pH 9.

In principle, cross-linking the core-forming PBzMA block should confer covalent stabilization and hence avoid this undesirable change in copolymer morphology on transfer into aqueous solution. Thus 10 mol % EGDMA was statistically copolymerized with the BzMA when generating the core-forming block. When targeting spherical nanoparticles, this copolymerization strategy worked well and produced cross-linked spheres. However, statistical copolymerization of EGDMA with BzMA when targeting block copolymer worms or vesicles resulted in the formation of insoluble gels. This is because the gradual branching of the core-forming block reduces the chain mobility, which is essential for the progressive evolution in copolymer morphology.[40] To prevent this gelation problem, the EGDMA cross-linker was added as a third short block after most of the BzMA comonomer had been consumed (as judged by ^{1}H NMR studies), so the desired copolymer morphology had already been achieved. Cross-linking was conducted for both spherical and vesicular particles (see Figures 5 and 6 respectively). Figure 6a shows PMAA$_{70}$-PBzMA$_{200}$ linear vesicles, while Figure 6b depicts the corresponding PMAA$_{70}$-PBzMA$_{200}$-PEGDMA$_{20}$ cross-linked vesicles. TEM studies of these cross-linked vesicles at pH 9 (Figure 6c) show no evidence for any (partial) worm formation, suggesting that covalent cross-linking has successfully stabilized the vesicular phase towards unwanted pH-induced morphological transitions.

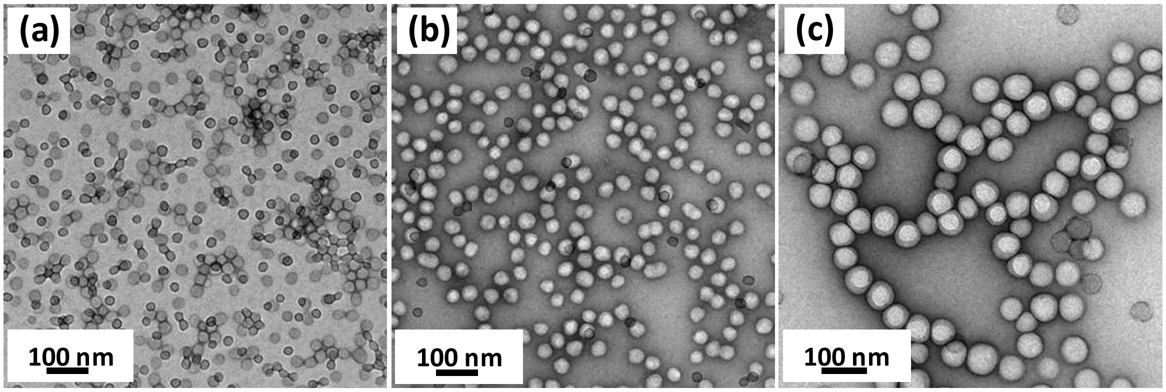

Figure 5. (a) PMAA$_{70}$-PBzMA$_{80}$ spherical particles before cross-linking; (b) corresponding PMAA$_{70}$-PBzMA$_{80}$-PEGDMA$_{8}$ spheres obtained after cross-linking (dried from ethanol); (c) the same PMAA$_{70}$-PBzMA$_{80}$-PEGDMA$_{8}$ cross-linked spheres transferred into alkaline aqueous solution (pH 9) prior to TEM sample preparation.

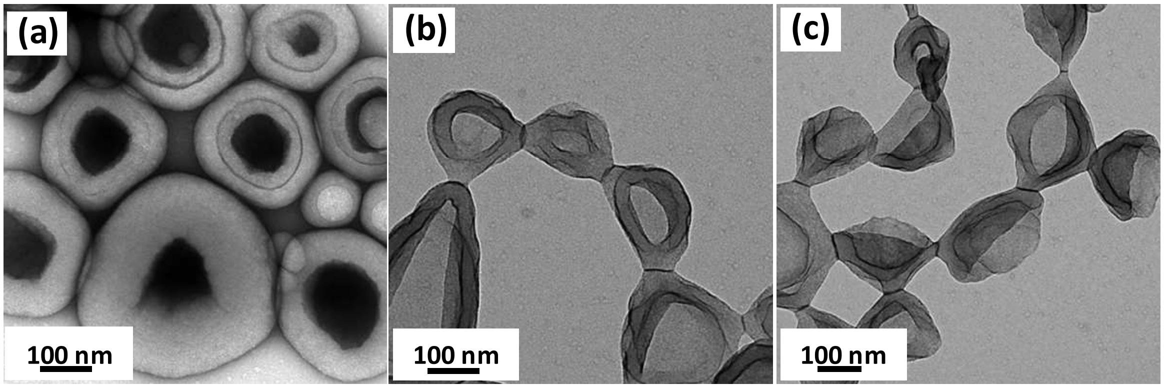

Figure 6. (a) $PMAA_{70}$-$PBzMA_{200}$ vesicles before cross-linking (b) $PMAA_{70}$-$PBzMA_{200}$-$PEGDMA_{20}$ vesicles after cross-linking (c) $PMAA_{70}$-$PBzMA_{200}$-$PEGDMA_{20}$ cross-linked vesicles at pH 9

We have previously shown that reasonably well-defined ABC triblock copolymers can be prepared via RAFT aqueous dispersion polymerization simply by adding a third monomer after full conversion of the second block.[40] More specifically, the chain extension of a poly(glycerol monomethacrylate)-poly(2-hydroxypropyl methacrylate) (PGMA-PHPMA) diblock copolymer using varying amounts of benzyl methacrylate led to the formation of a series of vesicles with a distinctive framboidal morphology, since the PBzMA block is enthalpically incompatible (immiscible) with the PHPMA block. Hence we decided to explore the feasibility of preparing ABC triblock copolymer nano-objects using the present RAFT alcoholic dispersion polymerization formulation.

In these experiments, a semi-fluorinated comonomer, 2,2,2-trifluoroethyl methacrylate (TFEMA), was selected to generate the second hydrophobic block (see Scheme 1). Thus a PMAA macro-CTA with a mean DP of 70 (M_n = 9,000 g mol^{-1}, M_w = 11,000 g mol^{-1}, M_w/M_n = 1.19) was first chain-extended using 100 units of BzMA (M_n = 22,450 g mol^{-1}, M_w = 28,100 g mol^{-1}, M_w/M_n = 1.25). TFEMA was added at 95% conversion, along with a second charge of initiator. In our initial attempts, ACVA initiator was utilized, which only resulted in 60% conversion being achieved after 24 h. This is because ACVA has poor solubility in the TFEMA monomer, hence the local concentration of this anionic initiator within the TFEMA-swollen micelle cores is rather low. In contrast, almost full conversion for the BzMA polymerization can be achieved within 24 h simply by replacing ACVA with neutral AIBN, which is much more soluble in TFEMA. The corresponding semi-log plot for the latter formulation indicates first-order kinetics with respect to monomer, see Figure 7.

The copolymer molecular weight increases linearly with conversion, indicating a well-controlled polymerization (see Figure 8). GPC analyses required exhaustive methylation of the PMAA block to render the block copolymers soluble in THF. Polydispersities remain below 1.45 throughout the polymerization. The GPC trace obtained for the PMAA-PBzMA diblock copolymer (see Figure 9) indicates a high blocking efficiency and minimal unreacted PMAA macro-CTA. The GPC traces obtained for the target $PMAA_{70}$-$PBzMA_{100}$-$PTFEMA_{300}$ triblock copolymer contain a shoulder that corresponds to the diblock copolymer precursor. This suggests sub-optimal blocking efficiency for the TFEMA polymerization (see Figure 9).

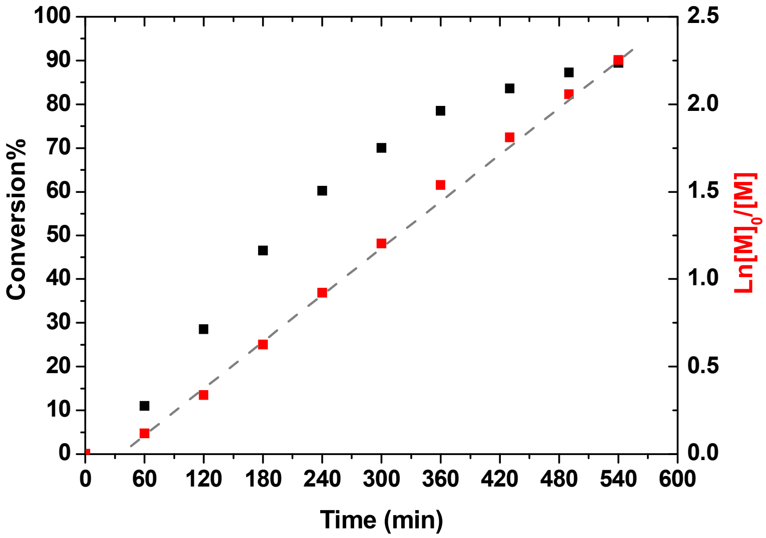

Figure 7. Kinetic data obtained at 70°C in ethanol for block extension of $PMAA_{70}$-$PBzMA_{100}$ with TFEMA at 20 % w/w. The targeted triblock composition was $PMAA_{70}$-$PBzMA_{100}$-$PTFEMA_{300}$.

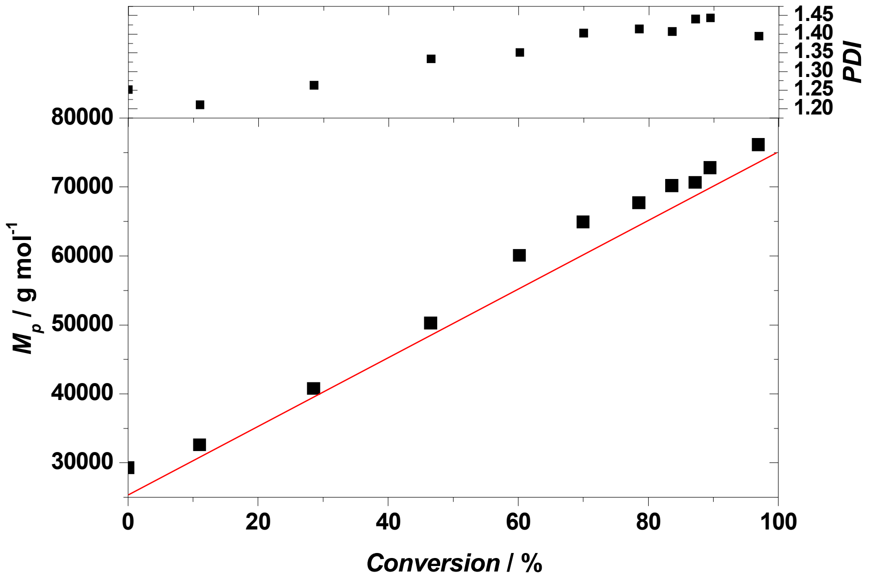

Figure 8. Evolution of number-average molecular weight M_p (vs. poly (methyl methacrylate) standards using THF GPC) and polydispersity (M_w/M_n) with monomer conversion for the RAFT dispersion polymerization of TFEMA in ethanol at 70°C. The targeted triblock composition was $PMAA_{70}$-$PBzMA_{100}$-$PTFEMA_{300}$ and the solids content was 20 % w/w.

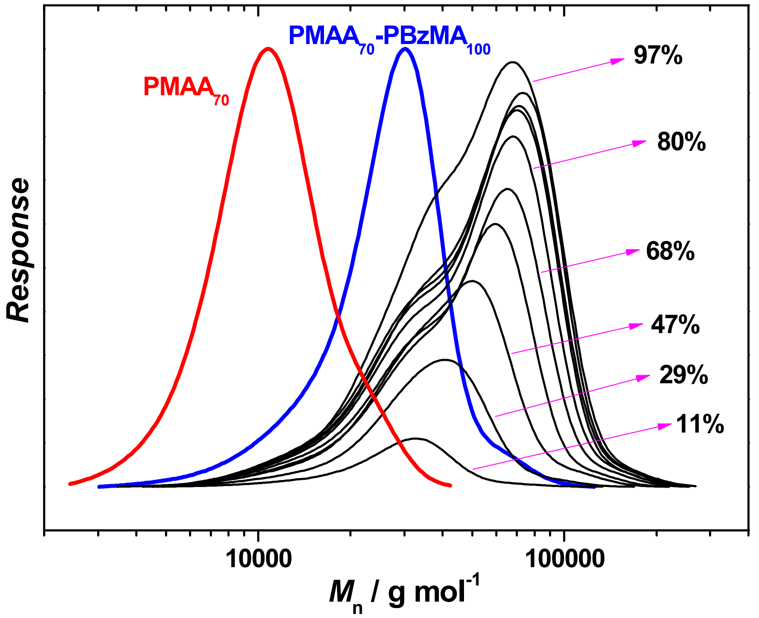

Figure 9. GPC traces (refractive index detector) recorded as a function of time during the RAFT seeded dispersion polymerization of TFEMA using a $PMAA_{70}$-$PBzMA_{100}$ macro-CTA at 70°C. The targeted triblock composition was $PMAA_{70}$-$PBzMA_{100}$-$PTFEMA_{300}$ and the solids content was 20 % w/w.

Prior to addition of the TFEMA monomer, the turbid reaction mixture was viscous and TEM studies confirm the presence of worm-like micelles (see Figure 10a). On addition of TFEMA, the reaction mixture was transformed into a clear transparent solution. This is because the TFEMA monomer acts as a co-solvent for the PBzMA chains. This monomer solvation effect is confirmed by TEM studies, which indicate the formation of spherical micelles of around 13 nm diameter (see Figure 1S). After a reaction time of 1 h (11 % TFEMA conversion; DP_{TFEMA}= 33,

Figure 10b) this mean diameter increases up to approximately 40 nm as judged by DLS. As the TFEMA polymerization proceeds further, the copolymer morphology evolves from spheres to worms and ultimately vesicles (see Figures 10c-k), as described in our previous studies.[36, 37, 39, 41, 42]

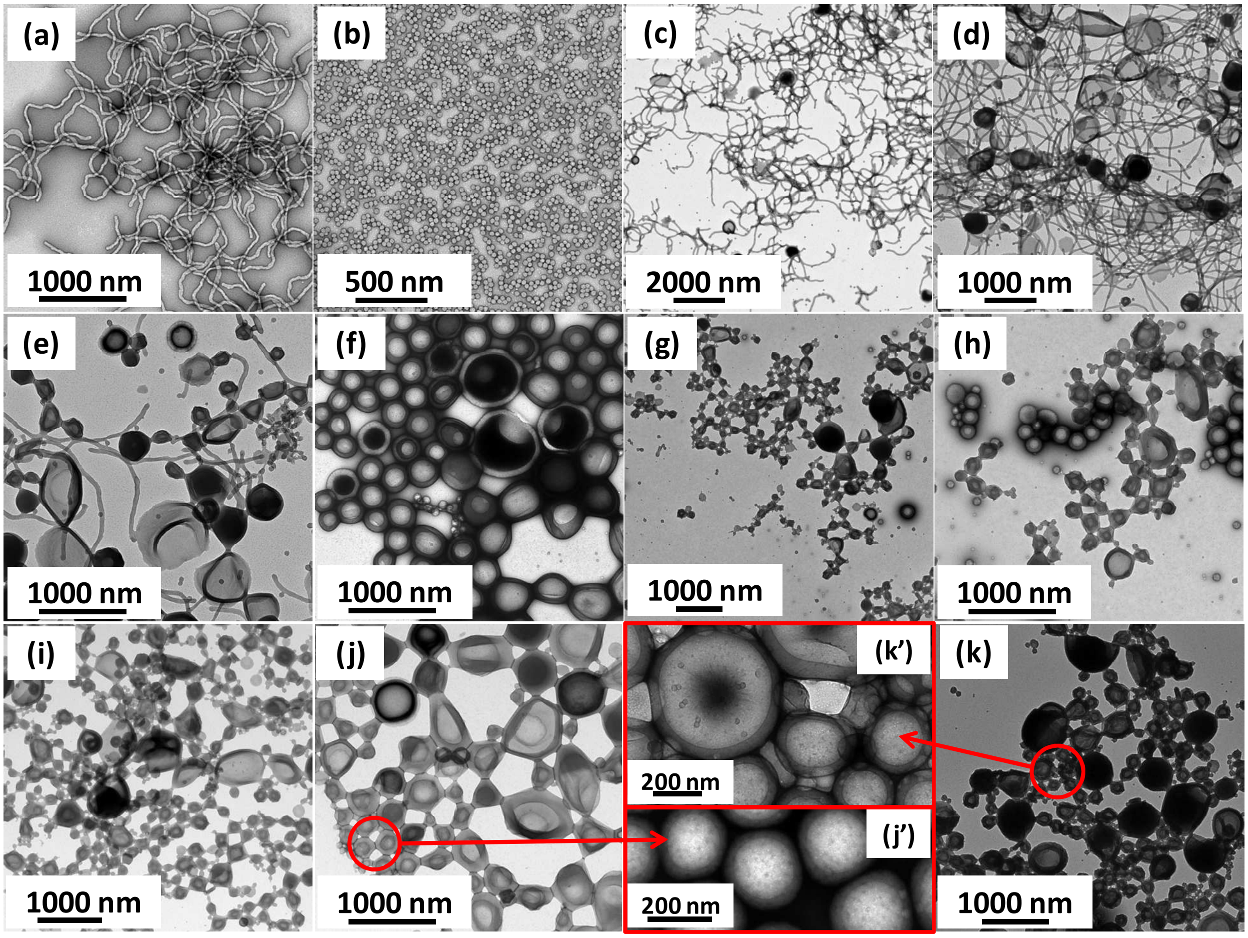

Figure 10. Representative TEM images obtained during the evolution of the PTFEMA block when targeting $PMAA_{70}$-$PBzMA_{100}$-$PTFEMA_x$, (a) initial $PMAA_{70}$-$PBzMA_{100}$ macro-CTA (x = 0); (b) after 1 h, x = 33; (c) after 2 h, x = 87; (d) after 3 h, x = 138; (e) after 4 h, x = 180; (f) after 5 h, x = 210; (g) after 6 h, x = 240; (h) after 7 h, x = 255; (i) after 8 h, x = 261; (j) after 9 h, x = 270; (k) after 24 h, x = 291. The targeted triblock composition was $PMAA_{70}$-$PBzMA_{100}$-$PTFEMA_{300}$.

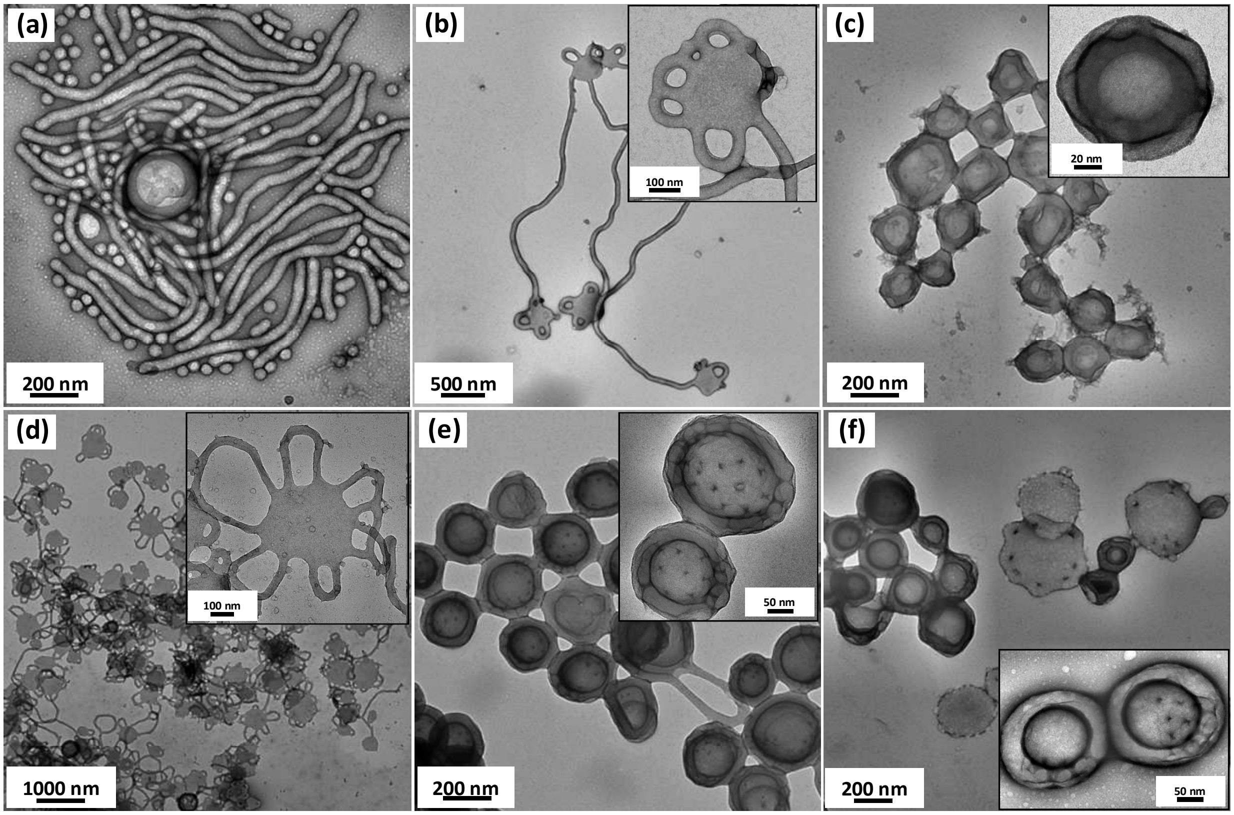

Figure 11. TEM images obtained for (a) $PMAA_{70}$-$PBzMA_{100}$-$PTFEMA_{100}$; (b) $PMAA_{70}$-$PBzMA_{200}$-$PTFEMA_{200}$; (c) $PMAA_{70}$-$PBzMA_{70}$-$PTFEMA_{223}$; (d) $PMAA_{70}$-$PBzMA_{191}$-$PTFEMA_{60}$; (e) $PMAA_{70}$-$PBzMA_{243}$-$PTFEMA_{60}$; (f) $PMAA_{70}$-$PBzMA_{273}$-$PTFEMA_{60}$.

Figure 11 shows TEM images recorded for various $PMAA_{70}$-$PBzMA_x$-$PTFEMA_y$ triblock compositions. A mixed phase of spheres, worms and vesicles is observed when x = y = 100 (see Figure 11a). Doubling the DP of each core-forming block results in worms that are interconnected via bilayer-type flat patches (see Figure 11b). Targeting a triblock composition of $PMAA_{70}$-$PBzMA_{70}$-$PTFEMA_{223}$ produces vesicles with phase- separated binary membranes (see Figure 11c). Flat bilayer patches with multiple worm loops are observed for $PMAA_{70}$-$PBzMA_{191}$-$PTFEMA_{60}$ in Figure 11d, while vesicles with perforated membranes are formed by $PMAA_{70}$-$PBzMA_{243}$-$PTFEMA_{60}$ and $PMAA_{70}$-$PBzMA_{273}$-$PTFEMA_{60}$ (see Figures 11e and 11f). During the evolution from worms to vesicles, partial coalescence occurs and bilayers are formed with protruding tentacles (see Figure 11b and 11d), as reported previously both for PGMA-PHPMA diblock copolymers prepared at high solids via PISA and also for binary mixtures of two amphiphilic diblock copolymers in dilute aqueous solution.[37,60] These structures then undergo ‘wrap up’ and form vesicles (see Figure 11c). In some cases, the wrap-up and fusion events are incomplete, which leads to surface porosity (see Figure 11e and 11f). These observations are consistent with recent transmission electron microscopy studies which suggest that branched worms first flatten to form pseudo-lamellae and then wrap up to form vesicles.[37,61]

Conclusions

Polymerization-induced self-assembly has been utilized to prepare a series of PMAA-PBzMA diblock copolymer nanoparticles via RAFT alcoholic dispersion polymerization of BzMA using a PMAA macro-CTA. Pure copolymer morphologies comprising spheres, worms or vesicles can be obtained, depending on the targeted diblock composition and the copolymer concentration. High monomer conversions, good blocking efficiencies and relatively low polydispersities were obtained in all cases. The resulting PMAA-PBzMA nano-objects acquire substantial anionic surface charge when transferred into aqueous solution due to ionization of the PMAA stabilizer chains. Vesicle dissociation to form worms and spheres occurs in aqueous alkaline solution, but covalently-stabilized vesicles remained intact under these conditions. Efficient chain extension of various PMAA-PBzMA diblock copolymer precursors was achieved using TFEMA to produce a range of remarkably complex semi-fluorinated triblock copolymer morphologies, with internal phase separation driven by the enthalpic incompatibility between the PBzMA and semi-fluorinated PTFEMA core-forming blocks.

References

(1) D. H. Solomon, E. Rizzardo, P. Cacioli, *US patent* 4 581 429, 1986.
(2) C. J. Hawker, A. W. Bosman, E. Harth, *Chem. Rev.*, 2001, **101**, 3661-3688.
(3) C. J. Hawker, *Handbook of Radical Polymerization*, John Wiley and Sons, Hoboken, 2002, 463-521.
(4) D. H. Solomon, *J. Polym. Sci. Pol. Chem.*, 2005, **43**, 5748-5764.
(5) M. Kato, M. Kamigaito, M. Sawamoto, T. Higashimura, *Macromolecules*, 1995, **28**, 1721-1723.
(6) J. S. Wang, K. Matyjaszewski, *J. Am. Chem. Soc.*, 1995, **117**, 5614-5615.
(7) K. Matyjaszewski, J. H. Xia, *Chem. Rev.*, 2001, **101**, 2921-2990.
(8) J. S. Wang, K. Matyjaszewski, *Macromolecules*, 1995, **28**, 7901-7910.
(9) V. Percec, B. Barboiu, *Macromolecules*, 1995, **28**, 7970-7972.
(10) E. Rizzardo, J. Chiefari, R. T. A. Mayadunne, G. Moad, S. H. Thang, *ACS Symp*. Ser., Controlled/Living Radical Polymerization: Progress in ATRP, NMP and RAFT, 2000, **768**, 278-296.
(11) A. Favier, M.-T. Charreyre, *Macromol. Rapid Commun.*, 2006, **27**, 653-692.

(12) G. Moad, E. Rizzardo, S. H. Thang, *Aust. J. Chem.*, 2006, **59**, 669-692.
(13) J. Chiefari, Y. K. Chong, F. Ercole, J. Krstina, J.Jeffery, C. L. Moad, G. Moad, E. Rizzardo, S. H. Thang, *Macromolecules*, 1998, **31**, 5559-5562.
(14) K. Matyjaszewski, *ACS Symp. Ser.*, Controlled/Living Radical Polymerization: Progress in ATRP, NMP and RAFT, 2000, **768**, 2-25.
(15) N. Hadjichristidis, S. Pispas, G. A. Floudas, *Block Copolymers*, 2003, New York, Wiley-Interscience, 1st Ed.
(16) I. W. Hamley, *The Physics of Block Copolymers*, 2003, Oxford University Press, 1st Ed.
(17) I. W. Hamley, *Developments in Block Copolymer Science and Technology*, 2005, Chicester, John Wiley & Sons Ltd, 1st Ed.
(18) P. C. Hiemenz, T. P. Lodge, *Polymer Chemistry*, 2007, USA, CRC Press, 2nd Ed.
(19) L. Zhang, A. Eisenberg, *J. Am. Chem. Soc.*, 1996, **118**, 3168.
(20) L. Zhang, A. Eisenberg, *Science,* 1995, **268**, 1728.
(21) B. M. Discher, Y. Y. Won, D. S. Ege, J. C. Lee, F. S. Bates, D. E. Discher, D. A. Hammer, *Science*, 1999, **284**, 1143-6.
(22) D. E. Discher, A. Eisenberg, *Science*, 2002, **297**, 967-973.
(23) S. Jain, F. S. Bates, *Science,* 2003, **300**, 460.
(24) S. Boissé, J. Rieger, K. Belal, A. Di-Cicco, P. Beaunier, M.-H. Li, B. Charleux, *Chem. Commun,.* 2010, **46**, 1950-1952.
(25) I. Chaduc, W. Zhang, J. Rieger, M. Lansalot, F. D'Agosto, B. Charleux, *Macromol. Rapid Commun.,* 2011, **32**, 1270-1276.
(26) B. Charleux, F. D'Agosto, G. Delaittre, *Adv. Polym. Sci.,* 2010, **233**, 125-183.
(27) B. Charleux, G. Delaittre, J. Rieger, F. D'Agosto, *Macromolecules,* 2012, **45**, 6753-6765.
(28) G. Delaittre, M. Save, M. Gaborieau, P. Castignolles, J. Rieger, B. Charleux, *Polym. Chem*., 2012, **3**, 1526-1538.
(29) E. Groison, S. Brusseau, F. D'Agosto, S. Magnet, R. Inoubli, L. Couvreur, B. Charleux, *ACS Macro Lett.,* 2011, **1**, 47-51.
(30) W. Zhang, F. D'Agosto, O. Boyron, J. Rieger, B. Charleux, *Macromolecules,* 2011, **44**, 7584-7593.
(31) W. Zhang, F. D'Agosto, O. Boyron, J. Rieger, B. Charleux, *Macromolecules,* 2012, **45**, 4075-4084.
(32) X. Zhang, S. Boisse, C. Bui, P.-A. Albouy, A. Brulet, M. H. Li, J. Rieger, B. Charleux, *Soft Matter,* 2012, **8**, 1130-1141.
(33) X. Zhang, S. P. Boissé, W. Zhang, P. Beaunier, F. D'Agosto, J. Rieger, B. Charleux, *Macromolecules,* 2011, **44**, 4149-4158.
(34) X. Zhang, J. Rieger, B. Charleux, *Polym. Chem*., 2012, **3**, 1502-1509.
(35) Y. Li, S. P. Armes, *Angew. Chem., Int. Ed.,* 2010, **49**, 4042-4046.
(36) S. Sugihara, A. Blanazs, S. P. Armes, A. J. Ryan, A. L. Lewis, *J .Am. Chem. Soc.*, 2011, **133**, 15707-15713.
(37) A. Blanazs, J. Madsen, G. Battaglia, A. J. Ryan, S. P. Armes, *J .Am. Chem. Soc.,* 2011, **133**, 16581-16587.
(38) M. Semsarilar, V. Ladmiral, A. Blanazs, S. P. Armes, *Langmuir,* 2011, **28**, 914-922.
(39) A. Blanazs, A. J. Ryan, S. P. Armes, *Macromolecules,* 2012, **45**, 5099-5107.
(40) P. Chambon, A. Blanazs, G. Battaglia, S. P. Armes, *Macromolecules*, 2012, **45**, 5081-5090.
(41) M. Semsarilar, E. R. Jones, A. Blanazs, S. P. Armes, *Adv. Mater.,* 2012, **24**, 3378-3382.
(42) L. Jones, M. Semsarilar, A. Blanazs, S. P. Armes, *Macromolecules,* 2012, **45**, 5091-5098.

(43) M. Semsarilar, V. Ladmiral, A. Blanazs, S. P. Armes, *Langmuir,* 2013*,* **29***,* 7416-7424.
(44) D. Zehm, L. Ratcliffe, S. P. Armes, *Macromolecules,* 2013, **46**, 128-139.
(45) G. Liu, Q. Qiu, W. Shen, Z. An, *Macromolecules,* 2011, **44**, 5237-5245.
(46) W. Shen, Y. Chang, G. Liu, H. Wang, A. Cao, Z. An, *Macromolecules,* 2011, **44**, 2524-2530.
(47) W. Cai, W. Wan, C. Hong, C. Huang, C.-Y. Pan, *Soft Matter,* 2010, **6**, 5554-5561.
(48) W.-D. He, X.-L. Sun, W.-M. Wan, C.-Y. Pan, *Macromolecules,* 2011, **44**, 3358-3365.
(49) C.-Q. Huang, C.-Y. Pan, *Polymer,* 2010, **51**, 5115-5121.
(50) W.-M. Wan, C.-Y. Pan, *Polymer Chemistry,* 2010, **1**, 1475-1484.
(51) L. Houillot, C. Bui, C. Farcet, C. Moire, J. A. Raust, H. Pasch, M. Save, B. Charleux, *ACS Appl. Mater. Interfaces,* 2010, **2**, 434.
(52) L. A. Fielding, M. Derry, V. Ladmiral, J. Rosselgong, A. M. Rodrigues, L. Ratcliffe, S. Sugihara, S. P. Armes, *Chem. Sci.*, 2013, **4**, 2081-2087
(53) Y. Inoue, J. Watanabe, M. Takai, S. Yusa, K. Ishihara, *J. Polym. Sci. Part A: Polym. Chem.,* 2005, **43**, 6073-6083.
(54) T.Y. Guo, D. Tang, M. Song, B. Zhang, *J.Polym. Sci. Part A: Polym. Chem.,* 2007, **45**, 5067-5075.
(55) N. M. L. Hansen, K. Jankova, S. Hvilsted, *Eur. Polym. J.*, 2007, **43**, 255-293.
(56) K. S. Pafiti, E. Loizou, C. S. Patrickios, L. Porcar, *Macromolecules* , 2010, **43**, 5195-5204.
(57) H. Peng, K. J. Thurecht, I. Blakey, E. Taran, A. K. Whittaker, *Macromolecules*, 2012, **45**, 8681-8690
(58) L. Couvreur, C. Lefay, J. Belleney, B. Charleux, O. Guerret, S. Magnet, *Macromolecules*, 2003, **36**, 8260-8267.
(59) J. Israelachvili, D. J. Mitchell, B. W. Ninham, *J. Chem. Soc., Faraday Trans. 2*, 1976, **72**, 1525-1568.
(60) S. Jain, F. S. Bates, *Macromolecules,* 2004, **37**, 1511-1523.
(61) L. Chen, H. W. Shen, A. Eisenberg, *J. Phys. Chem. B,* 1999, **103**, 9488-9497.

Graphical Abstract for:

Poly(methacrylic acid)-based AB and ABC Copolymer Nano-Objects prepared via RAFT Alcoholic Dispersion Polymerization

M. Semsarilar, V. Ladmiral, A. Blanazs and S. P. Armes*

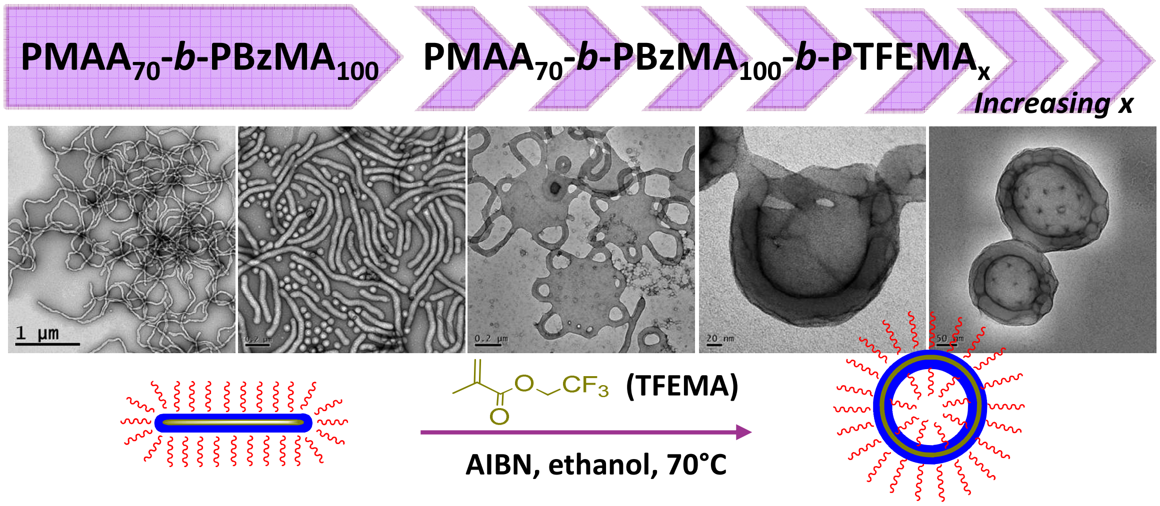

Graphical Abstract for PY ART 02 2014 000201:

Poly(methacrylic acid)-based AB and ABC Copolymer Nano-Objects prepared via RAFT Alcoholic Dispersion Polymerization

M. Semsarilar, V. Ladmiral, A. Blanazs and S. P. Armes*